

# Role of $\Lambda(1670)$ in $\gamma p \rightarrow K^+\eta\Lambda$ reaction near threshold

Li-Ye Xiao,<sup>1</sup> Qi-Fang Lü,<sup>2</sup> Ju-Jun Xie,<sup>3,4,5,\*</sup> and Xian-Hui Zhong<sup>1</sup>

<sup>1</sup>*Department of Physics, Hunan normal University, Changsha, Hunan 410081, China*

<sup>2</sup>*Department of Physics, Zhengzhou University, Zhengzhou, Henan 450001, China*

<sup>3</sup>*Institute of Modern Physics, Chinese Academy of Sciences, Lanzhou 730000, China*

<sup>4</sup>*Research Center for Hadron and CSR Physics, Institute of Modern Physics of CAS and Lanzhou University, Lanzhou 730000, China*

<sup>5</sup>*State Key Laboratory of Theoretical Physics, Institute of Theoretical Physics, Chinese Academy of Sciences, Beijing 100190, China*

(Dated: June 9, 2021)

The role of the  $\Lambda(1670)$  resonance in the  $\gamma p \rightarrow K^+\eta\Lambda$  reaction near threshold is studied within an effective Lagrangian approach. We perform a calculation for the total and differential cross section of the  $\gamma p \rightarrow K^+\eta\Lambda$  reaction by including the contributions from the  $\Lambda(1670)$  intermediate state decaying into  $\eta\Lambda$  dominated by  $K^-$  and  $K^{*-}$  mesons exchanges, the nucleon pole and  $N^*(1535)$  resonance decaying into  $K^+\Lambda$  dominated by exchanges of  $\omega$  and  $K^-$  mesons. Besides, the non-resonance process and contact terms to keep the total scattering amplitude gauge invariant are also considered. With our model parameters, the total cross section of this reaction is of the order of 1 nanobarn at photon beam energy  $E_\gamma \sim 2.5$  GeV. It is expected that our model predictions could be tested by future experiments.

PACS numbers: 13.75.-n.; 14.20.Gk.; 13.30.Eg.

## I. INTRODUCTION

One major goal of hadronic physics is to get the properties of baryon resonances. There exists a huge amount of data especially from  $\pi N$  reactions for studying the nucleon and  $\Delta(1232)$  resonances. The properties of most of these resonances are reliably extracted by analyzing various experimental data [1], which also can be reasonably described by the constituent quark models [2–4]. However, the situation changes when we look at the properties of  $\Lambda$  resonances. Large uncertainties exist due to poor statistic of data and limited knowledge of background contributions. Even for the well-established low-lying negative parity states, such as  $\Lambda(1405)$ ,  $\Lambda(1520)$ , and  $\Lambda(1670)$ , their properties are still controversial [5], although they are four-star ranking in the review of particle physics [1].

To uncover the puzzles in the  $\Lambda$  resonances, the  $K^-$ -induced reactions provide us an important tool, especially the reaction of  $K^-p \rightarrow \eta\Lambda$ . This reaction provides us a clear place to study the low-lying  $\Lambda$  resonances because only the  $\Lambda$  resonance contribute here due to the isospin selection rule. Thus, when some accurate data on the differential and total cross sections of the  $K^-p \rightarrow \eta\Lambda$  reaction were reported by the Crystal Ball Collaboration [6], they were analyzed with various theoretical models at once, e.g., effective Lagrangian model [7, 8], chiral quark model [9]. Recently, a comprehensive analysis of the  $K^-p$  scattering data of total and differential cross sections and recoil polarizations was performed with a dynamical coupled-channel model [10]. All of those the-

oretical analysis shows that the  $\Lambda(1670)$  dominates the  $K^-p \rightarrow \eta\Lambda$  reaction around threshold for its strong coupling to  $\eta\Lambda$ , while the other hyperon resonances give minor contributions.

In the present work, basing on the knowledge of the previous study of the  $K^-p \rightarrow \eta\Lambda$  reaction, we continue to study those  $\Lambda$  resonances from the  $\gamma p \rightarrow K^+\eta\Lambda$  process. This process is also an important tool to gain information on hadron resonance properties [11, 12]. In the  $\gamma p \rightarrow K^+\eta\Lambda$  process, the contributions of the  $\Lambda$  resonance diagrams are considered to be caused by the  $K^-$  and  $K^{*-}$  mesons exchanges between the initial photon and proton. While the  $\eta\Lambda$  production proceeds via the excitation of the intermediate  $\Lambda(1670)$ <sup>1</sup> resonance which has strong coupling to the  $\eta\Lambda$  channel.

The article is organized as follows. In the next section, the formalism and ingredients necessary for our estimations are presented, then we show our numerical results and discussions in Sect. III. Finally, a short summary is given in Sec. IV.

---

<sup>1</sup> It is worth to mention that within the coupled channel chiral perturbation theory, the  $\Lambda(1670)$  resonance is dynamically generated from the meson-baryon chiral interactions [13], which indicates that the nature of  $\Lambda(1670)$  could be meson-baryon molecular state. However, the structure of the  $\Lambda(1670)$  resonance is not the purpose of the present work. Hence, we will take it as an elementary particle considering its finite decay width in its propagator.

---

\*Electronic address: xiejujun@impcas.ac.cn

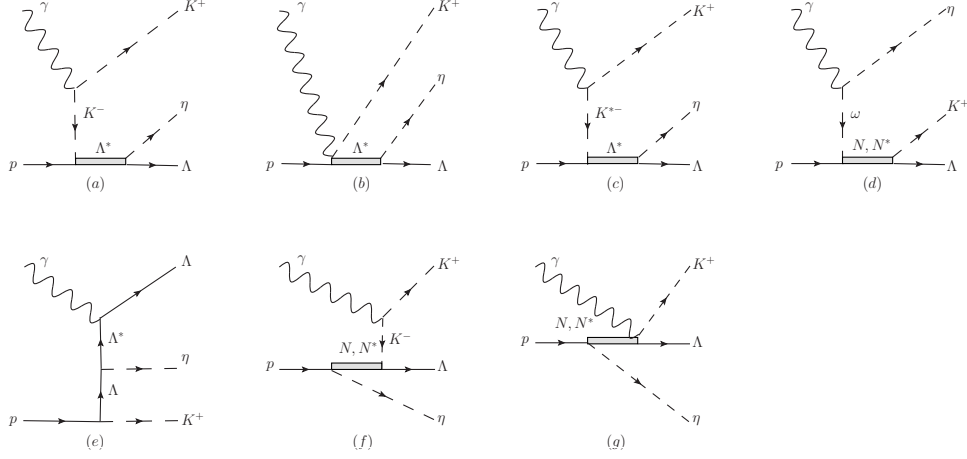


FIG. 1: Feynman diagrams for the  $\gamma p \rightarrow K^+ \eta \Lambda$  reaction.

## II. FORMALISM AND INGREDIENTS

We study the  $\gamma p \rightarrow K^+ \eta \Lambda$  reaction within an effective Lagrangian approach and the isobar model, which has been successfully used in our previous work [14–20]. The basic Feynman diagrams for this process are depicted in Fig. 1. Since  $\Lambda(1670)$  is close to the  $\eta\Lambda$  threshold and has strong coupling to  $\eta\Lambda$ , we pay attention to the contributions from the  $\Lambda(1670)$  ( $\equiv \Lambda^*$ ) resonance coupling to the  $\eta\Lambda$  final states. We also consider the contribution from  $N(1535)$  ( $\equiv N^*$ )<sup>2</sup> resonance which is caused by  $\omega$  exchange and decays into  $K^+\Lambda$  pair. It should be emphasized that the contact terms are required to keep the gauge invariant of the full scattering amplitude. In the calculations, we have ignored some diagrams, such as the diagrams of the  $\gamma p \rightarrow p(\text{or } N^*) \rightarrow K^+\Lambda(\text{or } \Lambda^*) \rightarrow K^+\eta\Lambda$  processes. The reason is that the couplings of the interaction vertexes involved in these diagrams are weaker than those diagrams we consider in Fig. 1 and the information of the interaction vertexes involved in these ignored diagrams is scarce.

To compute the contributions of the Feynman diagrams shown in Fig. 1, we adopt the interaction Lagrangian densities as used in Refs. [22, 23]:

$$\mathcal{L}_{\gamma KK} = e(K^- \partial^\mu K^+ - K^+ \partial^\mu K^-) A_\mu, \quad (1)$$

$$\mathcal{L}_{\gamma KK^*} = \frac{eg_{\gamma KK^*}}{m_{K^*}} \varepsilon^{\mu\nu\alpha\beta} \partial_\mu K_\nu^* \partial_\alpha A_\beta K, \quad (2)$$

$$\mathcal{L}_{\gamma\eta\omega} = \frac{eg_{\gamma\eta\omega}}{m_\omega} \varepsilon^{\mu\nu\alpha\beta} \partial_\mu \omega_\nu \partial_\alpha A_\beta \eta, \quad (3)$$

$$\mathcal{L}_{\gamma\Lambda\Lambda^*} = \frac{e\kappa_{\gamma\Lambda\Lambda^*}}{2(m_\Lambda + m_{\Lambda^*})} \bar{\Lambda}^* \gamma_5 \sigma_{\mu\nu} \Lambda F^{\mu\nu} + \text{h.c.}, \quad (4)$$

$$\mathcal{L}_{K\Lambda\Lambda^*} = g_{K\Lambda\Lambda^*} \bar{N} K \Lambda^* + \text{h.c.}, \quad (5)$$

$$\mathcal{L}_{K\Lambda N^*} = g_{K\Lambda N^*} \bar{\Lambda} K N^* + \text{h.c.}, \quad (6)$$

$$\mathcal{L}_{\eta\Lambda\Lambda^*} = g_{\eta\Lambda\Lambda^*} \bar{\Lambda} \eta \Lambda^* + \text{h.c.}, \quad (7)$$

$$\mathcal{L}_{\eta NN^*} = g_{\eta NN^*} \bar{N} \eta N^* + \text{h.c.}, \quad (8)$$

$$\mathcal{L}_{K^* N \Lambda^*} = g_{K^* N \Lambda^*} \bar{N} \gamma_5 \gamma^\mu K_\mu^* \Lambda^* + \text{h.c.}, \quad (9)$$

$$\mathcal{L}_{\omega NN} = g_{\omega NN} \bar{N} (\gamma_\mu + \frac{\kappa_{\omega NN}}{2m_N} \sigma_{\mu\nu} \partial^\nu) \omega^\mu N, \quad (10)$$

$$\mathcal{L}_{\omega NN^*} = g_{\omega NN^*} \bar{N} \gamma_5 \gamma^\mu \omega_\mu N^* + \text{h.c.}, \quad (11)$$

$$\mathcal{L}_{K\Lambda N} = -\frac{g_{K\Lambda N}}{m_N + m_\Lambda} \bar{\Lambda} \gamma_5 \gamma_\mu \partial^\mu K N, \quad (12)$$

$$\mathcal{L}_{\eta NN} = -\frac{g_{\eta NN}}{2m_N} \bar{N} \gamma_5 \gamma_\mu \partial^\mu \eta N, \quad (13)$$

where  $e = \sqrt{4\pi\alpha}$  ( $\alpha$  is the fine-structure constant),  $A_\mu$  and  $F_{\mu\nu} (= \partial_\mu A_\nu - \partial_\nu A_\mu)$  are the photon field and electromagnetic field tensor, respectively. We take  $\kappa_{\omega NN} = 0$  as used in Ref. [24] and  $\kappa_{\gamma NN^*} = 2.06$  obtained from the partial decay width of  $N^* \rightarrow N\gamma$ . For  $\kappa_{\gamma\Lambda\Lambda^*}$ , we determine it with  $SU(3)$  flavor symmetry prediction, which gives  $\kappa_{\gamma\Lambda\Lambda^*} = 1.03$ .<sup>3</sup> For the coupling value  $g_{\omega NN}$ , with the ratio of  $g_{\omega NN}/g_{\rho NN} = 3.0$  [24], and the value of  $g_{\rho NN} \simeq 3.36$  [14], we get  $g_{\omega NN} \simeq 10.09$ . For the coupling constants  $g_{N^* N \omega}$  and  $g_{\Lambda^* N K^*}$ , they are also obtained with the  $SU(3)$  flavor symmetry relation, which gives  $g_{N^* N \omega} \simeq 0.43$  and  $g_{\Lambda^* N K^*} \simeq 0.75$ .<sup>4</sup> Moreover, we take  $g_{\eta NN} = 2.02$  and  $g_{K\Lambda N} = -13.98$  as used in Ref. [17], while the other coupling constants are deter-

<sup>2</sup> We ignore the contributions from other low-lying s-wave nucleon resonances which have small contributions to the present calculation according to the Moorhouse selection rules [21], which pointed that those nucleon resonances have very weak or vanish  $\gamma NN^*$  coupling and hence have weak  $\omega NN^*$  coupling.

<sup>3</sup> Obtained with the relation  $\kappa_{\gamma NN^*}/\kappa_{\gamma\Lambda\Lambda^*} = 2$  which was predicted by a chiral quark model [25].

<sup>4</sup> Obtained with  $g_{N^* N \rho} = 0.87$  [15],  $g_{N^* N \rho}/g_{N^* N \omega} = 2$  and  $g_{\Lambda^* N K^*}/g_{N^* N \omega} = \sqrt{3}$ , which is evaluated from the vector meson-quark couplings using a chiral quark model [25].

mined from the partial decay width of  $K^*$ ,  $\omega$ ,  $\Lambda(1670)$ , and  $N(1535)$  as listed in Tab I.

TABLE I: Parameters used in the present calculations. [FS] means that the corresponding parameters are obtained from the  $SU(3)$  flavor symmetry.

State	Width (MeV)	Decay channel	Adopted branching ratio	$g^2/4\pi$
$K^*$	51	$\gamma K$	$9.9 \times 10^{-6}$	$2.24 \times 10^{-2}$
$\omega$	8	$\gamma\eta$	$4.6 \times 10^{-6}$	$9.75 \times 10^{-3}$
$\Lambda(1670)$	35	$\bar{K}N$	0.25	$9.20 \times 10^{-3}$
		$\Lambda\eta$	0.18	$6.59 \times 10^{-2}$
		$\bar{K}^*N$	—	$4.48 \times 10^{-2}$ [FS]
		$\gamma\Lambda$	—	$8.44 \times 10^{-2}$ [FS]
$N(1535)$	150	$N\eta$	0.42	0.28
		$\Lambda K$	—	$6.88 \times 10^{-2}$ [23]
		$N\omega$	—	$1.50 \times 10^{-2}$ [FS]

The propagators of nucleon (or  $\Lambda$  hyperon), vector mesons  $\omega$  and  $K^{*-}$ , and pseudo-scalar  $K^-$  meson can be written in the forms of

$$G_{N/\Lambda}(p_{N/\Lambda}) = i \frac{\not{p}_{N/\Lambda} + m_{N/\Lambda}}{p_{N/\Lambda}^2 - m_{N/\Lambda}^2}, \quad (14)$$

$$G_V^{\mu\nu}(p_V) = -i \frac{g^{\mu\nu} - p_V^\mu p_V^\nu / m_V^2}{p_V^2 - m_V^2}, \quad (15)$$

$$G_K(p_K) = \frac{i}{p_K^2 - m_K^2}, \quad (16)$$

where  $p_{N/\Lambda}$ ,  $p_V$ , and  $p_K$  are the four-momentum of the exchanged nucleon (or  $\Lambda$  hyperon), vector mesons  $\omega$  and

$K^{*-}$ , and pseudo-scalar  $K^-$  meson, respectively.

In addition, the propagators for  $\Lambda(1670)$  and  $N(1535)$  can be written in a Breit-Wigner form [26],

$$G_R(p_R) = \frac{i(\not{p}_R + M_R)}{p_R^2 - M_R^2 + iM_R\Gamma_R}, \quad (17)$$

where  $p_R$ ,  $M_R$ , and  $\Gamma_R$  are the four-momentum, mass and the total decay width of  $\Lambda(1670)$  or  $N(1535)$ , respectively.

Besides, we need to include the form factors because the hadrons are not point-like particles. We adopt here the common scheme used in many previous works. In our calculations, the form factors for  $K$ ,  $K^*$ ,  $\omega$ , off-shell nucleon pole,  $N(1535)$ , off-shell  $\Lambda$  pole, and  $\Lambda^*$  are adopted the form advocated in Refs. [18, 27–29],

$$F(p_{ex}^2, M_{ex}) = \left[ \frac{\Lambda_c^4}{\Lambda_c^4 + (p_{ex}^2 - M_{ex}^2)^2} \right]^n, \quad (18)$$

with  $p_{ex}$  and  $M_{ex}$  the four-momentum and mass of exchanged hadron, respectively,  $\Lambda_c$  the so-called cutoff parameter and  $n = 1$  or  $2$  depending on the specific coupling [30]. In the calculation, we adopt  $n = 1$  for  $K$ ,  $N(1535)$ , and  $\Lambda(1670)$ , while  $n = 2$  for  $K^*$ ,  $\omega$ , nucleon pole, and  $\Lambda$  pole. Besides, to minimize the number of free parameters, we use the same cut off parameters  $\Lambda_c = 1.5$  GeV for all the exchanged hadrons for simplicity.

With those established effective Lagrangians, propagators, and coupling constants, the invariant scattering amplitudes for the  $\gamma p \rightarrow K^+ \eta \Lambda$  reaction can be obtained straightforwardly by following the standard Feynman rules. The amplitudes for Fig. 1, can be written as

$$\mathcal{M}_a = eg_{\eta\Lambda\Lambda^*}g_{\bar{K}N\Lambda^*}F(p_K^2, m_K)F(p_{\Lambda^*}^2, m_{\Lambda^*})\bar{u}(p_5, s_5)G_{\Lambda^*}(p_{\Lambda^*})u(p_2, s_2)G_K(p_K)(p_3^\mu - p_K^\mu)\varepsilon_\mu(p_1, s_1), \quad (19)$$

$$\mathcal{M}_b = eg_{\eta\Lambda\Lambda^*}g_{\bar{K}N\Lambda^*}F(p_K^2, m_K)F(p_{\Lambda^*}^2, m_{\Lambda^*})\bar{u}(p_5, s_5)G_{\Lambda^*}(p_{\Lambda^*})\frac{p_{\Lambda^*}^\mu}{p_1 \cdot p_{\Lambda^*}}u(p_2, s_2)\varepsilon_\mu(p_1, s_1), \quad (20)$$

$$\begin{aligned} \mathcal{M}_c &= \frac{eg_{\eta\Lambda\Lambda^*}g_{\bar{K}^*N\Lambda^*}g_{\gamma KK^*}F(p_{K^*}^2, m_{K^*})F(p_{\Lambda^*}^2, m_{\Lambda^*})}{m_{K^*}}\bar{u}(p_5, s_5)G_{\Lambda^*}(p_{\Lambda^*})\gamma_5(\gamma_\lambda - \frac{p_{\Lambda^*}\lambda\cancel{p}_{\Lambda^*}}{p_{\Lambda^*}^2})u(p_2, s_2) \\ &\times G_{K^*}^{\lambda\nu}(p_{K^*})\varepsilon_{\mu\nu\alpha\beta}p_{K^*}^\mu p_1^\alpha \varepsilon^\beta(p_1, s_1), \end{aligned} \quad (21)$$

$$\mathcal{M}_d^N = \frac{eg_{K\Lambda N}g_{\omega NN}g_{\gamma\eta\omega}F(p_\omega^2, m_\omega)F(p_N^2, m_N)}{(m_5 + m_N)m_\omega}\bar{u}(p_5, s_5)\gamma_5\cancel{p}_3G_N(p_N)\gamma_\lambda u(p_2, s_2)G_\omega^{\lambda\nu}(p_\omega)\varepsilon_{\mu\nu\alpha\beta}p_\omega^\mu p_1^\alpha \varepsilon^\beta(p_1, s_1), \quad (22)$$

$$\begin{aligned} \mathcal{M}_d^{N^*} &= \frac{eg_{K\Lambda N^*}g_{\omega NN^*}g_{\gamma\eta\omega}F(p_\omega^2, m_\omega)F(p_{N^*}^2, m_{N^*})}{m_\omega}\bar{u}(p_5, s_5)G_{N^*}(p_{N^*})\gamma_5(\gamma_\lambda - \frac{p_{N^*}\lambda\cancel{p}_{N^*}}{p_{N^*}^2})u(p_2, s_2) \\ &\times G_\omega^{\lambda\nu}(p_\omega)\varepsilon_{\mu\nu\alpha\beta}p_\omega^\mu p_1^\alpha \varepsilon^\beta(p_1, s_1), \end{aligned} \quad (23)$$

$$\mathcal{M}_e = \frac{ek_{\gamma\Lambda\Lambda^*}g_{\eta\Lambda\Lambda^*}g_{K N\Lambda}F(p_{\Lambda^*}^2, m_{\Lambda^*})F(p_\Lambda^2, m_\Lambda)}{(m_5 + m_{\Lambda^*})(m_2 + m_\Lambda)}\bar{u}(p_5, s_5)\gamma_5\gamma^\mu\varepsilon_\mu(p_1, s_1)G_{\Lambda^*}(p_{\Lambda^*})G_\Lambda(p_\Lambda)\gamma_5\cancel{p}_3u(p_2, s_2), \quad (24)$$

$$\mathcal{M}_f^N = \frac{eg_{K\Lambda N}g_{\eta NN}F(p_K^2, m_K)F(p_N^2, m_N)}{(m_5 + m_N)(m_2 + m_N)}\bar{u}(p_5, s_5)\gamma_5\cancel{p}_K G_N(p_N)\gamma_5\cancel{p}_4 G_K(p_K)(p_3^\mu - p_K^\mu)\varepsilon_\mu(p_1, s_1), \quad (25)$$

$$\mathcal{M}_f^{N^*} = eg_{K\Lambda N^*}g_{\eta NN^*}F(p_K^2, m_K)F(p_{N^*}^2, m_{N^*})\bar{u}(p_5, s_5)G_{N^*}(p_{N^*})u(p_2, s_2)G_K(p_K)(p_3^\mu - p_K^\mu)\varepsilon_\mu(p_1, s_1), \quad (26)$$

$$\mathcal{M}_g^N = \frac{eg_{K\Lambda N}g_{\eta NN}F(p_K^2, m_K)F(p_N^2, m_N)}{(m_5 + m_N)(m_2 + m_N)}\bar{u}(p_5, s_5)\frac{\gamma_5(\cancel{p}_1 - \cancel{p}_3)p_3^\mu}{p_1 \cdot p_3}G_N(p_N)\gamma_5\cancel{p}_4u(p_2, s_2)\varepsilon_\mu(p_1, s_1), \quad (27)$$

$$\mathcal{M}_g^{N^*} = eg_{K\Lambda N^*}g_{\eta NN^*}F(p_K^2, m_K)F(p_{N^*}^2, m_{N^*})\bar{u}(p_5, s_5)\frac{p_K^\mu}{p_1 \cdot p_K}G_{N^*}(p_{N^*})u(p_2, s_2)\varepsilon_\mu(p_1, s_1), \quad (28)$$

where the sub-indices  $a, b, c, d, e, f,$  and  $g$  stand for the diagrams shown in Fig. 1. The  $p_1, p_2, p_3, p_4$  and  $p_5$  represent the four-momentums of the photon, proton,  $K^+$  meson,  $\eta$  meson and  $\Lambda$  hyperon, respectively. The  $s_1, s_2$  and  $s_5$  are the spin projections of the photon, proton and  $\Lambda$  hyperon, respectively.  $p_K$  and  $p_{K^*}$  ( $= p_1 - p_3$ ) correspond to the four-momentum of exchanged  $K^-$  and  $K^{*-}$  meson, respectively.  $p_\omega$  ( $= p_1 - p_4$ ) is the four-momentum of exchanged  $\omega$  meson.  $p_\Lambda$  ( $= p_2 - p_3$ ) is the four-momentum of exchanged  $\Lambda$  hyperon.  $p_N$  and  $p_{N^*}$  ( $= p_2 - p_4$ ) are the four-momentum of intermediate nucleon and nucleon resonances, respectively.  $p_{\Lambda^*}$  ( $= p_4 + p_5$ ) (Fig. 1 (a), (b) and (c)) and  $p'_{\Lambda^*}$  ( $= p_1 - p_5$ ) (Fig. 1 (e)) are the four-momentum of the intermediate  $\Lambda(1670)$  resonance.

The contact terms illustrated in Fig. 1 (b) and (g) serve to keep the full amplitude ( $\mathcal{M}$ ) gauge invariant. By including the amplitude  $\mathcal{M}_b$  and  $\mathcal{M}_g^{N, N^*}$ , it is easy to show that the total amplitude satisfies the gauge invariance

$$p_1 \cdot \mathcal{M} = 0 \quad (29)$$

with

$$\begin{aligned} \mathcal{M} &= \mathcal{M}_a + \mathcal{M}_b + \mathcal{M}_c + \mathcal{M}_d^N + \mathcal{M}_d^{N^*} + \mathcal{M}_e \\ &+ \mathcal{M}_f^N + \mathcal{M}_f^{N^*} + \mathcal{M}_g^N + \mathcal{M}_g^{N^*}. \end{aligned} \quad (30)$$

Finally, the cross section for  $\gamma p \rightarrow K^+\eta\Lambda$  reaction can be calculated with

$$\begin{aligned} d\sigma(\gamma p \rightarrow K^+\eta\Lambda) &= \frac{1}{8E_\gamma} \sum_{s_1, s_2, s_5} |\mathcal{M}|^2 \frac{d^3p_3}{2E_3} \frac{d^3p_4}{2E_4} \frac{m_\Lambda d^3p_5}{E_5} \\ &\times \delta^4(p_1 + p_2 - p_3 - p_4 - p_5), \end{aligned} \quad (31)$$

where  $E_3, E_4,$  and  $E_5$  are the energies of the final particles  $K^+, \eta,$  and  $\Lambda$  hyperon, respectively;  $E_\gamma$  is the energy of incident photon at laboratory frame.

### III. NUMERICAL RESULTS AND DISCUSSIONS

In this section we show our theoretical results of the total and differential cross sections of the  $\gamma p \rightarrow K^+\eta\Lambda$  reaction near  $\eta$ -meson production threshold.

### A. Total cross section

The total cross section versus excess energy  $E_\gamma$  for the  $\gamma p \rightarrow K^+ \eta \Lambda$  reaction is calculated by using a Monte Carlo multi-particle phase space integration program. In Fig. 2, we plot the total cross section as a function of the photon beam energy  $E_\gamma$  in the region of  $2.0 < E_\gamma < 2.5$  GeV. From Fig. 2, one can clearly see that the  $\Lambda(1670)$  resonance [i.e., the contributions from the diagrams (a), (b), and (c) in Fig. 1] gives a dominant contribution to the reaction from the threshold to  $E_\gamma = 2.5$  GeV, while the contributions from the other diagrams shown in Fig. 1 are small.

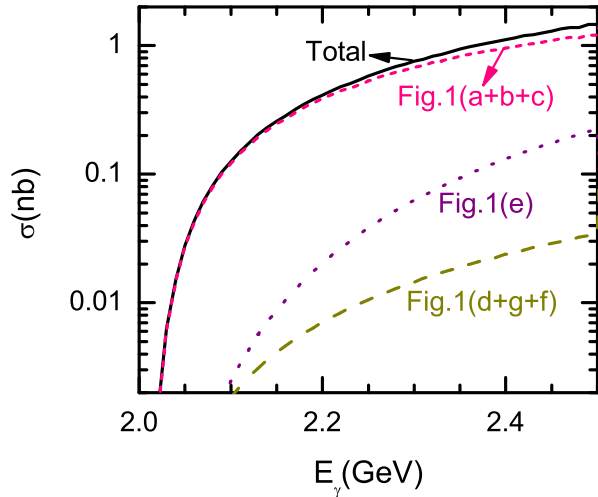


FIG. 2: (Color online) The cross sections vs photon beam energy ( $E_\gamma$ ) for the  $\gamma p \rightarrow K^+ \eta \Lambda$  reaction from present calculation obtained with the parameters in the table I. The solid curve represents the total cross sections including all the contributions of Fig. 1. Different contributions of Fig. 1 (a+b+c), Fig. 1 (e) and Fig. 1 (d+f+g) are indicated explicitly by the legends in the figures.

The contribution of the  $\Lambda(1670)$  resonance includes three parts: (i)  $K^-$  meson exchange [Fig. 1 (a)]; (ii) contact term [Fig. 1 (b)]; and (iii)  $K^{*-}$  vector meson exchange [Fig. 1 (c)]. The relative importance of these three process to the  $\gamma p \rightarrow K^+ \eta \Lambda$  reaction is obviously shown in Fig. 3. From which we can see that the contribution from  $K^{*-}$  vector meson exchange is larger than that from  $K^-$  meson exchange between the reaction threshold and  $E_\gamma \approx 2.16$  GeV. But, with increase of photon energies  $E_\gamma$ , the contribution from  $K^-$  meson exchange grows faster than the one from  $K^{*-}$  vector meson exchange. This can be easily understood since the value of the coupling constant  $g_{\bar{K}^* N \Lambda(1670)}^2$  obtained according to the  $SU(3)$  flavor symmetry is about 5 times larger than  $g_{\bar{K} N \Lambda(1670)}^2$  determined from the partial decay width of  $\Lambda(1670) \rightarrow \bar{K} N$ . Thus, the contribution from  $K^{*-}$  vec-

tor meson exchange is dominant around the threshold. However, with the photon energy increasing, the contribution of  $K^-$  exchange is to become more important for the faster increase of the contribution from the  $K^-$  exchange. The contribution from contact term is small in the whole energy region considered in the present work.

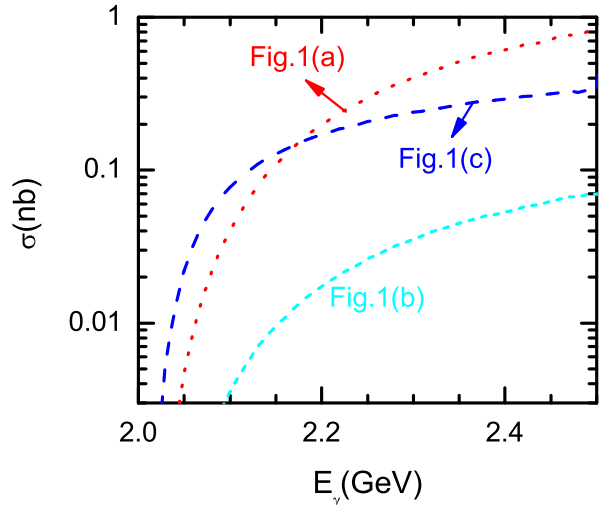


FIG. 3: (Color online) The cross sections vs photon beam energy ( $E_\gamma$ ) for the  $\gamma p \rightarrow K^+ \eta \Lambda$  reaction from  $\Lambda(1670)$  resonance contribution. The contributions of  $K^-$  meson exchange [Fig. 1 (a)],  $K^{*-}$  vector-meson exchange [Fig. 1 (c)] and contact term [Fig. 1 (b)] are indicated with red dotted line, blue dashed line and cyan short dashed line, respectively.

Meanwhile, due to the uncertainty of the form factors, it is necessary to consider the effects of form factors on the cross sections. For the dominant contributions of  $\Lambda(1670)$  to the reaction, we just need consider the influence of the form factors on the cross section from the  $K^{*-}$ - and  $K^-$ -exchanges.

Firstly, we consider the form factors effects on the cross section with different values of  $n$  ( $n=1$  or  $n=2$ ) by fixing the cutoff parameter with  $\Lambda_c = 1.5$  GeV. The results are shown in Fig. 4. We can see that the cross section is sensitive to  $n$ . With  $n=2$  the cross section is obviously suppressed compared with that of  $n=1$ . The difference between the cross section predicted with  $n=1$  and that predicted with  $n=2$  becomes more and more large with the photon energy  $E_\gamma$  increasing. For example, at photon energy  $E_\gamma = 2.5$  GeV the cross section for  $K^-$  exchange varies from 0.5 nb to 0.8 nb with the values of  $n$  changed from 2 to 1. While, for  $K^{*-}$  exchange, the cross section varies from 0.3 nb to 0.7 nb.

Next, we consider the form factors effects on the cross sections with different cutoff parameters  $\Lambda_c$ . In Fig. 5, we show the predicted cross sections of the  $K^-$  and  $K^{*-}$  exchanges with three typical cutoff parameters  $\Lambda_c = 1.2, 1.5, 1.8$  GeV, respectively. From the figure, it clearly see that the predicted cross sections have

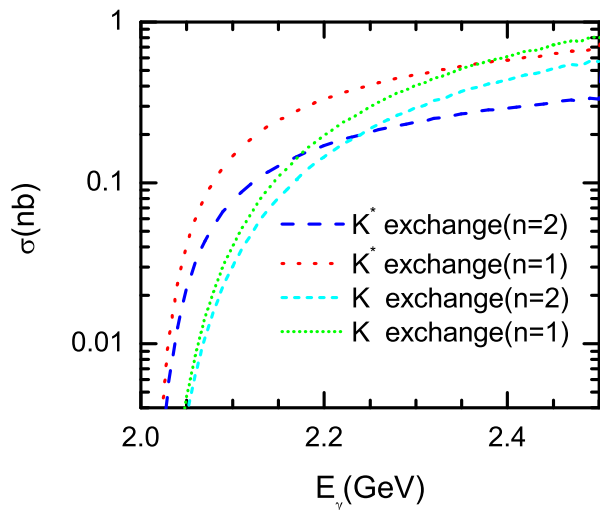


FIG. 4: (Color online) The cross sections vs photon beam energy ( $E_\gamma$ ) for the  $\gamma p \rightarrow K^+ \eta \Lambda$  reaction from  $K^-$  and  $K^{*-}$  meson-exchanges contributions with the different values of  $n$  with cutoff parameter  $\Lambda_c = 1.5$  GeV.

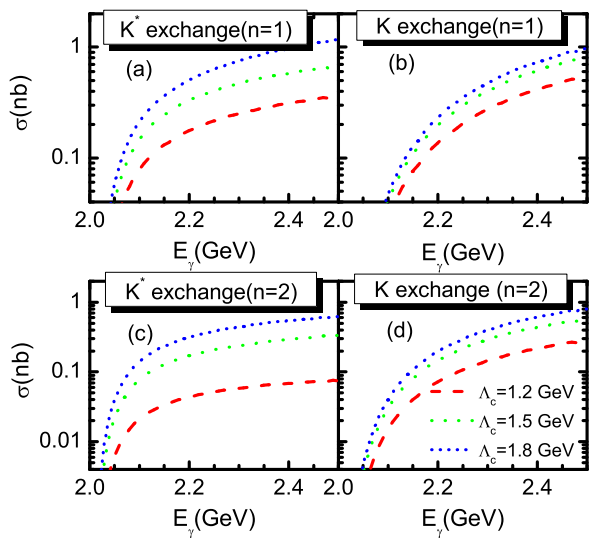


FIG. 5: (Color online) (a)-(b): the cross sections vs photon beam energy ( $E_\gamma$ ) for the  $\gamma p \rightarrow K^+ \eta \Lambda$  reaction from the exchanged  $K^-$  and  $K^{*-}$  mesons contributions with the different values of cutoff parameter  $\Lambda_c$  with  $n = 1$ ; (c)-(d): as in (a)-(b) but with  $n = 2$ .

a strong dependence on the cutoff parameter  $\Lambda_c$ . Considering a 20% uncertainty of the cutoff parameter, i.e.,  $\Lambda_c = 1.5 \pm 0.3$  GeV, we find that the uncertainty of the predicted cross sections can reach to 100% – 200%.

Finally, it should be pointed out that our results might bear some uncertainties from the coupling constant  $g_{\Lambda(1670)K^*N}$ , since it is estimated from the  $SU(3)$  flavor symmetry. However, there is no experimental data on

this reaction, we will leave those issues to further studies in the future.

As a whole, with our model parameters,  $\Lambda(1670)$  with exchanged  $K^-$  and  $K^{*-}$  mesons gives the dominant contribution to the  $\gamma p \rightarrow K^+ \eta \Lambda$  reaction, while the contributions from nucleon,  $N(1535)$  resonance and  $t$ -channel are negligibly small. The form factors have large effects on the total cross section.

## B. Differential cross section

In addition to the total cross section, we also study the differential cross section for  $\gamma p \rightarrow K^+ \eta \Lambda$  reaction. The corresponding momentum distribution and angular distribution of outgoing  $K^+$  meson,  $\eta$  meson, and hyperon  $\Lambda$ , the  $K\Lambda$  and  $\eta\Lambda$  invariant mass spectrum in the center-of-mass frame at two energy points  $E_\gamma = 2.1, 2.4$  GeV are shown in Fig. 6 and Fig. 7, respectively.

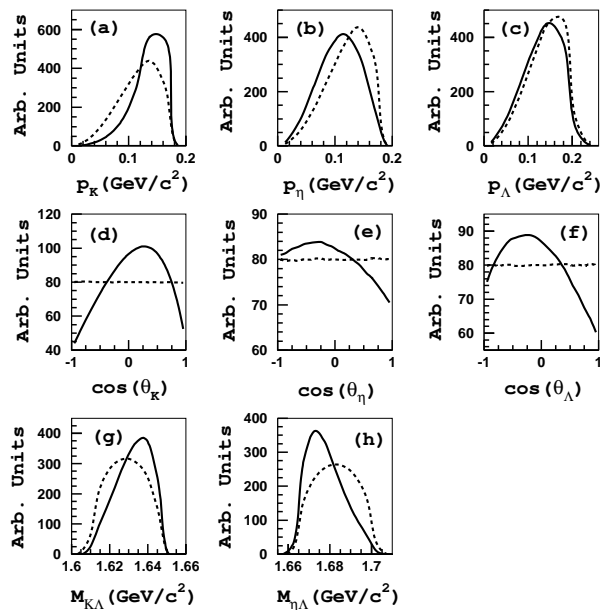


FIG. 6: Difference cross sections (solid lines) for the  $\gamma p \rightarrow \eta \Lambda K^+$  at the excess energy  $E_\gamma = 2.1$  GeV and phase-space distribution (dashed lines). (a)-(c): the momentum distribution of outgoing  $K^+$  meson,  $\eta$  meson and hyperon  $\Lambda$ , respectively; (d)-(f): the angular distribution of the  $K^+$  meson,  $\eta$  meson and hyperon  $\Lambda$  in the total center-of-mass frame, respectively; (g)-(h): the invariant mass spectrum of the outgoing hyperon  $\Lambda$  and  $K^+$  meson, outgoing  $\Lambda$  and  $\eta$  meson, respectively.

From the figures, we see that the  $K^+$  meson and  $\eta$  meson momentum distributions are very different from the results with phase space only. However, the  $\Lambda$  hyperon momentum distributions is similar to the results with

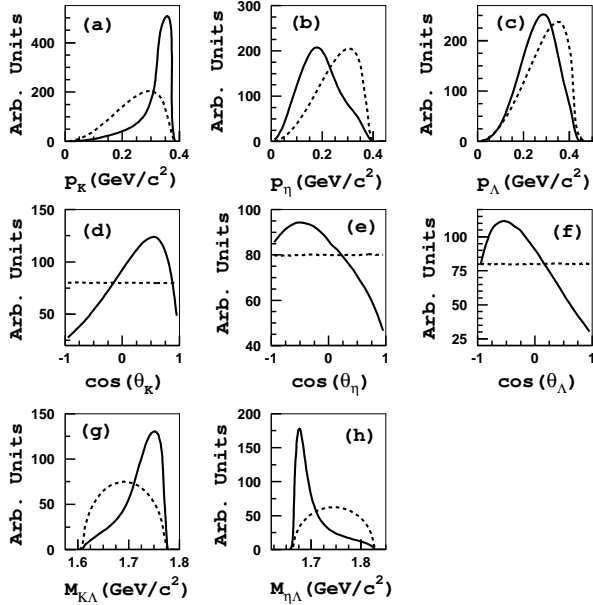


FIG. 7: As in Fig. 6 but for the case of  $E_\gamma = 2.4$  GeV.

phase space only. Furthermore, from the angular distributions shown in the figures, we see that  $K^+$  meson has a large distribution at forward angles. While the  $\eta$  meson and hyperon  $\Lambda$  have large distributions at the backward angles. Finally, from the  $\eta\Lambda$  invariant mass spectrum, it is seen a obvious peak at  $M_{\eta\Lambda} \approx 1.675$  GeV, which is from the contribution of  $\Lambda(1670)$ .

It should be pointed out that the effective Lagrangian approach is a convenient tool to catch the qualitative features of the  $\gamma p \rightarrow K^+\eta\Lambda$  reaction; however, it is not consistent with the unitary requirements. In principle, the

unitary is important for extracting the parameters of the baryon resonances from the experimental data [31, 32], especially for those processes involving many intermediate couple channels and three-particle final states [33, 34]. Thus, the unitary might introduce effects on our model predictions. Meanwhile, couple channel effects can not be taken into account in our calculations. Our model calculation constitutes the first step in this direction.

#### IV. SUMMARY AND CONCLUSIONS

In this work, we investigate the total and differential cross sections of the  $\gamma p \rightarrow K^+\eta\Lambda$  reaction within an effective Lagrangian model. It is shown that the resonant diagrams induced by  $K^{*-}$  and  $K^-$  mesons provide the most important contributions. It is also found that the contributions from nucleon pole and  $N(1535)$  due to the  $\omega$  meson exchange and  $K$  meson exchange are negligibly small. It should be remarked the form factors for exchanged  $K^{*-}$  vector meson and exchanged  $K^-$  meson have a significant effect on the cross section.

We also studied the differential cross section at beam energy  $E_\gamma = 2.1, 2.4$  GeV. It is found that  $K^+$  meson has forward angle distribution, while  $\eta$  meson and hyperon  $\Lambda$  have backward angle distribution. We expect that future experiments will provide a test to our model calculations.

#### Acknowledgments

This work is partly supported by the National Natural Science Foundation of China (Grants No. 11475227, No. 11075051 and No. 11375061), the Hunan Provincial Natural Science Foundation (Grant No. 13JJ1018), and the Hunan Provincial Innovation Foundation for Postgraduate.

- 
- [1] K. A. Olive *et al.* [Particle Data Group Collaboration], *Chin. Phys. C* **38**, 090001 (2014).  
[2] N. Isgur and G. Karl, *Phys. Rev. D* **18**, 4187 (1978).  
[3] S. Capstick and N. Isgur, *Phys. Rev. D* **34**, 2809 (1986).  
[4] U. Loring, B. C. Metsch and H. R. Petry, *Eur. Phys. J. A* **10**, 395 (2001).  
[5] E. Klempt and J. M. Richard, *Rev. Mod. Phys.* **82**, 1095 (2010).  
[6] A. Starostin *et al.* [Crystal Ball Collaboration], *Phys. Rev. C* **64**, 055205 (2001).  
[7] B. C. Liu and J. J. Xie, *Phys. Rev. C* **86**, 055202 (2012).  
[8] B. C. Liu and J. J. Xie, *Phys. Rev. C* **85**, 038201 (2012).  
[9] L. Y. Xiao and X. H. Zhong, *Phys. Rev. C* **88**, 065201 (2013).  
[10] H. Kamano, S. X. Nakamura, T.-S. H. Lee and T. Sato, *Phys. Rev. C* **90**, 065204 (2014).  
[11] C. Hanhart, *Phys. Rept.* **397**, 155 (2004).  
[12] B. S. Zou, *Chin. Phys. C* **33**, 1113 (2009), and references therein.  
[13] C. Garcia-Recio, J. Nieves, E. Ruiz Arriola and M. J. Vicente Vacas, *Phys. Rev. D* **67**, 076009 (2003).  
[14] J. J. Xie and B. S. Zou, *Phys. Lett. B* **649**, 405 (2007).  
[15] J. J. Xie, B. S. Zou and H. C. Chiang, *Phys. Rev. C* **77**, 015206 (2008).  
[16] J. J. Xie, E. Wang and J. Nieves, *Phys. Rev. C* **89**, 015203 (2014).  
[17] J. J. Xie, B. C. Liu and C. S. An, *Phys. Rev. C* **88**, 015203 (2013).  
[18] C. Z. Wu, Q. F. Lü, J. J. Xie and X. R. Chen, *Commun. Theor. Phys.* **63**, no. 2, 215 (2015).  
[19] J. J. Xie, J. J. Wu and B. S. Zou, *Phys. Rev. C* **90**, 055204 (2014).  
[20] J. J. Xie, E. Wang and B. S. Zou, *Phys. Rev. C* **90**, 025207 (2014).  
[21] R. G. Moorhouse, *Phys. Rev. Lett.* **16**, 772 (1966).  
[22] W. T. Chiang, S. N. Yang, M. Vanderhaeghen and

- D. Drechsel, Nucl. Phys. A **723**, 205 (2003).
- [23] B. C. Liu, Phys. Rev. C **86**, 015207 (2012).
- [24] D. O. Riska and G. E. Brown, Nucl. Phys. A **679**, 577 (2001).
- [25] Q. Zhao, Z. p. Li and C. Bennhold, Phys. Rev. C **58**, 2393 (1998).
- [26] W. H. Liang, P. N. Shen, J. X. Wang and B. S. Zou, J. Phys. G **28**, 333 (2002).
- [27] T. Feuster and U. Mosel, Phys. Rev. C **58**, 457 (1998); *ibid.* **59**, 460 (1999).
- [28] G. Penner and U. Mosel, Phys. Rev. C **66**, 055211 (2002); *ibid.* **66**, 055212 (2002).
- [29] V. Shklyar, H. Lenske and U. Mosel, Phys. Rev. C **72**, 015210 (2005).
- [30] R. Machleidt, K. Holinde and C. Elster, Phys. Rept. **149**, 1 (1987).
- [31] H. Kamano, B. Julia-Diaz, T. -S. H. Lee, A. Matsuyama and T. Sato, Phys. Rev. C **80**, 065203 (2009).
- [32] N. Suzuki, B. Julia-Diaz, H. Kamano, T. -S. H. Lee, A. Matsuyama and T. Sato, Phys. Rev. Lett. **104**, 042302 (2010).
- [33] H. Kamano, B. Julia-Diaz, T. -S. H. Lee, A. Matsuyama and T. Sato, Phys. Rev. C **79**, 025206 (2009).
- [34] H. Kamano, S. X. Nakamura, T. S. H. Lee and T. Sato, Phys. Rev. D **84**, 114019 (2011).